

# Phase II basket trial of Dual Anti-CTLA-4 and anti-PD-1 blockade in Rare Tumors (DART) SWOG S1609: pancreatic neuroendocrine neoplasm (PNEN) cohort

Sandip Pravin Patel <sup>1</sup>, Jillian Fisher,<sup>2</sup> Young Kwang Chae <sup>3</sup>, Luisa Solis Soto,<sup>4</sup> Anup Kasi,<sup>5</sup> Bhavana Konda,<sup>6</sup> Mark Walshauer,<sup>7</sup> Edwin Parra,<sup>4</sup> Jiexin Zhang,<sup>8</sup> Caroline Duault <sup>9</sup>, Edgar Gonzalez-Kozlova,<sup>10</sup> Ganiraju Manyam,<sup>11</sup> Jianhua Zhang,<sup>12</sup> Hong Chen,<sup>11</sup> Dzifa Yawa Duose,<sup>11</sup> Caddie Laberiano Fernandez,<sup>11</sup> Raja Luthra,<sup>11</sup> Gheath Al-Atrash,<sup>11</sup> Seunghee Kim-Schulze,<sup>13</sup> Holden T Maecker,<sup>14</sup> Ignacio I Wistuba,<sup>11</sup> Sacha Gnjatic,<sup>15</sup> J Jack Lee <sup>8</sup>, Jianjun Zhang <sup>16</sup>, Christine M Magner,<sup>17</sup> Helen X Chen,<sup>18</sup> Elad Sharon,<sup>19</sup> Megan Othus <sup>20</sup>, Christopher W Ryan,<sup>21</sup> Charles Blanke,<sup>21</sup> Cara L Haymaker <sup>4</sup>, Razelle Kurzrock<sup>22</sup>

**To cite:** Patel SP, Fisher J, Chae YK, *et al.* Phase II basket trial of Dual Anti-CTLA-4 and anti-PD-1 blockade in Rare Tumors (DART) SWOG S1609: pancreatic neuroendocrine neoplasm (PNEN) cohort. *Journal for ImmunoTherapy of Cancer* 2025;**13**:e011760. doi:10.1136/jitc-2025-011760

► Additional supplemental material is published online only. To view, please visit the journal online (<https://doi.org/10.1136/jitc-2025-011760>).

SPP, YKC and RK contributed equally.  
CLH and RK contributed equally.

Accepted 06 June 2025



© Author(s) (or their employer(s)) 2025. Re-use permitted under CC BY-NC. No commercial re-use. See rights and permissions. Published by BMJ Group.

For numbered affiliations see end of article.

## Correspondence to

Dr Sandip Pravin Patel;  
spatel@ucsd.edu

## ABSTRACT

**Purpose** SWOG S1609 Dual Anti-CTLA-4 and anti-PD-1 blockade in Rare Tumors (DART) studied the efficacy of ipilimumab combined with nivolumab across multiple rare tumor types. We report the results of the pancreatic neuroendocrine neoplasm (PNEN) cohort.

**Experimental design** Treatment consisted of ipilimumab 1 mg/kg intravenously every 6 weeks with nivolumab 240 mg intravenously every 2 weeks. The primary endpoint was overall response rate (ORR) (Response Evaluation Criteria In Solid Tumors RECIST V.1.1). Secondary endpoints include progression-free survival (PFS), overall survival (OS), and toxicity. Clinical benefit rate (includes ORR plus stable disease (SD) >6 months) was examined. Correlative studies were performed. The trial was conducted by the National Cancer Institute/Southwest Oncology Group Early Therapeutics and Rare Cancers Committee and opened at >1,000 sites.

**Results** 19 patients with PNEN were enrolled. The median number of lines of prior therapy was 2 (range: 0–4). The ORR was 11% (2/19 patients); the clinical benefit rate (CBR; stable disease >6 months+partial response+complete response), 26% (5/19). The median PFS was 3 months; median OS, 24 months. The longest PFSs were 26 (intermediate grade PNEN), 31 (low grade) and 39+ months (intermediate grade). The most common toxicities were fatigue (47% of patients) and aspartate aminotransferase (AST) elevation (32%); the most common grade 3/4 immune-related adverse event (AE) was AST (32%) and bilirubin elevation (26%), with no grade 5 events. Programmed death-ligand 1 expression by chromogenic immunohistochemistry (N=12 patients assessed) did not associate with ORR; tumor mutation burden (TMB) was high in three patients; one of the two patients with partial remission (PFS=26 months) had high

## WHAT IS ALREADY KNOWN ON THIS TOPIC

⇒ Pancreatic neuroendocrine neoplasms are rare tumors with low response rates to anti-programmed cell death protein-1 immunotherapy

## WHAT THIS STUDY ADDS

⇒ Nivolumab combined with low-dose ipilimumab demonstrated a clinical benefit rate (includes stable disease >6 months plus objective response) of 26% with durable benefit lasting >2 years in 3 of 19 patients.

## HOW THIS STUDY MIGHT AFFECT RESEARCH, PRACTICE OR POLICY

⇒ These results suggest that dual immunotherapy may be useful for a subset of patients with this rare cancer and that additional investigations are warranted.

TMB (150 mutations/mb). Peripheral effector memory T-cell activation (N=11 patients assessed by cytometry by time-of-flight with 5 having longitudinal analysis) was associated with response, though the number of patients evaluated was limited.

**Conclusions** Low-dose ipilimumab plus nivolumab demonstrated an 11% ORR and 26% CBR (includes SD >6 months) in patients with refractory PNEN, with durable benefit (>2 years) in 3 (16%) patients.

**Trial registration number** NCT02834013.

## INTRODUCTION

Immune checkpoint blockade has had a dramatic effect on improving outcomes across multiple cancer types, including in

rare tumors such as anal cancer and Merkel cell carcinoma.<sup>1,2</sup> Less is known about the benefit of anti-cytotoxic T-lymphocyte associated protein 4 (CTLA-4) and anti-programmed cell death protein-1 (PD-1) approaches in other rare cancers. SWOG 1609 DART (Dual Anti-CTLA-4 and anti-PD-1 blockade in Rare Tumors), a federally (National Cancer Institute (NCI)) funded basket immunotherapy study investigating ipilimumab with nivolumab in rare cancers was launched to address this unmet medical need. The trial investigated low-dose ipilimumab and regular-dose nivolumab across 53 rare tumor types (though one cohort received nivolumab alone), with signals of efficacy in multiple histologies including but not limited to angiosarcoma, anaplastic thyroid cancer, small bowel carcinoma, and metastatic breast cancer.<sup>3–7</sup>

We have also previously reported S1609 results across all grades of non-pancreatic neuroendocrine neoplasms (PNEN), with a 44% overall response rate (ORR) in patients with high-grade disease, versus a 0% ORR in patients with lower-grade tumors.<sup>8</sup> A separate, prospective high-grade neuroendocrine neoplasm cohort was launched within S1609 showing a 26% ORR overall, including one of two patients with poorly-differentiated, high-grade pancreatic neuroendocrine cancer with a complete remission lasting over 3 years.<sup>9</sup>

We report here the results of a distinct cohort of PNEN across grade and differentiation, including higher-grade pancreatic neuroendocrine carcinoma and pancreatic neuroendocrine tumors (PNETs).

## PATIENTS AND METHODS

The trial was conducted by the Early Therapeutics and Rare Cancers Committee of Southwest Oncology Group (SWOG), and the investigational agents were provided by the Cancer Therapy Evaluation Program of the NCI under an NCI Cooperative Research and Development Agreement (CRADA) agreement with Bristol-Myers Squibb. The protocol and all amendments were approved by SWOG, the NCI, the NCI Central Institutional Review Board, and by the regulatory committees at the participating institutions (ClinicalTrials.gov NCT02834013). All study subjects provided their voluntary, written informed consent, and the study was conducted in accordance with the Declaration of Helsinki.

### Rationale for population

Rare cancers for S1609 were selected based on a reported incidence of less than 6 in 100,000 per year.<sup>10</sup> Local pathology review was used, with pathology report review by the SWOG study team. PNEN grading was based on 2019 WHO criteria.

### Patient selection

Patients were required to be >18 years of age, have an Eastern Cooperative Oncology Group (ECOG)/Zubrod performance status of 0–2, with absolute neutrophil count  $\geq 1 \times 10^9/L$ , platelets  $\geq 75,000/mcL$ , hemoglobin  $\geq$

**Table 1** Patient characteristics (median (minimum, maximum) or N (%) reported; N=19 patients)

Factor	Summary, n=19
Age (years)	62 (18–75)
Performance status	
0	8 (42)
1	11 (58)
Ethnicity	
Hispanic	0
Not Hispanic	19 (100)
Race	
Black	1 (5)
White	18 (95)
Grade	
High	5 (26)
Intermediate	7 (37)
Low	4 (21)
Not reported	3 (16)
Differentiation	
Poorly differentiated	2 (11)
Well-differentiated	8 (42)
Not reported	9 (47)
Number of prior regimens	2 (0, 4)

80 g/L, creatinine clearance  $\geq 50$  mL/min, total bilirubin  $\leq 2.0 \times$  institutional upper limit of normal (IULN), aspartate aminotransferase (AST) and alanine aminotransferase (ALT)  $\leq 3.0 \times$  IULN, TSH or free T4 serum  $\leq$  IULN, and adrenocorticotrophic hormone (ACTH)  $\leq$  IULN. Women of childbearing potential were required to have a negative serum pregnancy test, and participants were required to practice adequate birth control during protocol participation.

Tumor grade and differentiation were based on local pathology and the WHO 2019 classification and grading of PNEN was used at the time of study accrual. Individual characteristics are summarized in [table 1](#).

### Treatment and monitoring

Treatment consisted of ipilimumab 1 mg/kg intravenously every 6 weeks with nivolumab 240 mg intravenously every 2 weeks until disease progression, symptomatic deterioration, treatment delay for any reason >56 days, unacceptable or immune-related toxicity with inability to decrease prednisone to <10 mg daily, or per patient request.

Patients were evaluated with a history and physical, and toxicity assessment at least every 6 weeks with the beginning of each cycle. Laboratory evaluation included complete blood count, comprehensive metabolic panel, thyroid stimulating hormone, free thyroxine, ACTH, cortisol, lipase. Imaging studies by CT for disease assessment were performed pre-study, week 8, week 16, week 24, and then every 12 weeks until progression.

## Statistical methods and outcomes

The primary objective was to evaluate the ORR (confirmed complete and partial responses (CR and PR)) by Response Evaluation Criteria In Solid Tumors (RECIST) V.1.1 based on local RECIST assessment. A two-stage design was used to evaluate a true  $ORR \leq 5\%$  (null hypothesis, as patients had failed all known active therapies) versus  $\geq 30\%$  (alternative hypothesis, a potentially clinically meaningful difference in tumor response in refractory solid tumors). The first stage sample size was 6 patients; if  $>1$  had a response (confirmed CR or PR), an additional 10 patients were to be accrued. The design specified that 2 or more responses out of 16 patients would reject the null hypothesis (one-sided  $\alpha=13\%$ ,  $power=87\%$ ). The secondary objectives were to estimate progression-free survival (PFS), overall survival (OS), ORR by immune-related RECIST (iRECIST), PFS by iRECIST, and toxicity assessment by Common Terminology Criteria for Adverse Events (CTCAE) V.4.0. We also assessed the clinical benefit rate (CBR) (stable disease (SD) $>6$  months/PR/CR).

PFS was measured from the start of protocol therapy to the first date of progression by RECIST V.1.1 or death by any cause, with patients last known to be alive without progression censored at the date of last contact. OS was measured from the date of study registration to the date of death by any cause, with patients last known to be alive censored at the date of last contact. PFS and OS estimates were calculated using the Kaplan-Meier method. CIs for medians were constructed using the method of Brookmeyer and Crowley.<sup>11</sup> CIs for the primary ORR analysis accounted for the two-stage design and observed sample size.<sup>12</sup> All analyses were performed using R V.4.2.1.

## Translational analyses

### Samples for translational analysis

RNA and DNA were extracted from archival or baseline paraffin tumor tissue provided by the SWOG bank, along with slides cut from the same block for image analysis. Peripheral blood mononuclear cells (PBMCs) and plasma were provided by the SWOG bank and assessed longitudinally at baseline, cycle 2 week 9 (C2W9) and at progression. The number of samples available for analysis is shown in online supplemental figure 1.

### NanoString gene expression assay

RNA extracted from baseline formalin-fixed paraffin-embedded (FFPE) samples enrolled in the S1609 trial was received from the SWOG bank ( $n=7$ ). Samples were run on the nCounter platform using the nCounter PanCancer Immune Profiling panel (730 immune-related and 40 housekeeping genes) (<https://nanosttring.com/products/ncounter-assays-panels/oncology/pancancer-immune-profiling/>) (per manufacturer's instructions). Briefly, samples were hybridized overnight at  $65^{\circ}\text{C}$  to probes, excess probes were washed using the automated prep station and then imaged on the digital analyzer. All runs included a Human Reference RNA control for batch

correction. Data were processed and normalized with NanoString's nSolver analysis software. All samples passed the post-run QC metrics and no batch effects were evident in the runs. B-cell scores were derived using TIMER.

### Whole-exome sequencing data analysis

Whole-exome sequencing (WES) analysis was conducted using the CIDC WES pipeline on tumor DNA from nine tumors that passed quality control. DNA from paired peripheral blood mononuclear samples was used as a germ line control ( $n=4$ ). WES implements Gene Analysis Toolkit<sup>13</sup> best practices and identifies somatic variants using Sentieon TNScope and Haplotyper algorithms,<sup>14</sup> respectively. Somatic variants are annotated using the Variant Effect Predictor software.<sup>15</sup> The pipeline uses an ensemble of three callers, CNVkit,<sup>16</sup> Sequenza,<sup>17</sup> and Facets,<sup>18</sup> to characterize tumor copy number variation (CNV), and the CNV segments called by at least two callers were used to generate a high-confident consensus set. Sequenza and FACETS were used to estimate tumor purity and also PyClone-VI was used to infer clonal status of mutations.<sup>19</sup> PyClone V.0.13.1<sup>20</sup> was used to perform mutation clonality analysis. It is a Bayesian clustering method that enables mutations to be grouped into putative clonal clusters by integrating copy number, tumor purity (obtained from Sequenza), and variant allele frequency data.

### Immunohistochemistry for PD-L1

Immunohistochemistry (IHC) was used to assess the expression of programmed death-ligand 1 (PD-L1) in tumor tissue ( $n=12$ ). The optimal conditions were previously validated.<sup>21</sup> We used the Leica Bond Max autostainer system (Leica Biosystems) with standard Leica protocol, which is briefly described here: FFPE tissue sections were deparaffinized and rehydrated; then, antigen retrieval was performed with Bond ER2 (Leica Biosystems, pH 9.0 Cat# AR9640) for 20 min; the primary antibody (PD-L1; clone 28–8, dilution 1:100; Abcam) was incubated for 15 min at room temperature and detected using the Bond Polymer Refine Detection kit (Leica Biosystems) with 3,3'-diaminobenzidine as the chromogen; finally, the slides were counterstained with hematoxylin, dehydrated and cover-slipped. Positive (placenta) and negative (diluent) controls were used in each run. Two pathologists assessed PD-L1 staining expression in the membrane of viable malignant cells and reported the percentage of malignant cells with any positive PD-L1 membrane staining (Tumor Proportion Score). For this purpose, samples were considered adequate for IHC evaluation if they contained  $\geq 100$  viable tumor cells.

### Multiplex immunofluorescence staining and analysis

Multiplex immunofluorescence (mIF) staining ( $n=12$ ) was performed using similar methods and reagents previously described and validated.<sup>22</sup> Briefly, sequential 4  $\mu\text{m}$ -thick FFPE tumor sections were stained using an automated staining system (BOND-RX; Leica Microsystems,

Buffalo Grove, Illinois, USA) placed in two mIF panel contained: Panel 1, cytokeratin (clone AE1/AE3, cat# M351501-2, dilution 1:300, Dako, Santa Clara, California, USA), PD-L1 (clone E1L3N, cat# 13684S, dilution 1:3,000, Cell Signaling Technology, Danvers, Massachusetts, USA), CD68 (clone PG-M1, cat# M087601-2, dilution 1:450, Dako), CD3 (polyclonal, cat#IS503, dilution 1:100, Dako), CD8 (clone C8/144B, cat# MS-457-S, dilution 1:300, Thermo Fisher Scientific, Waltham, Massachusetts, USA), and PD-1 (clone EPR4877-2, cat# ab137132, dilution 1:250, Abcam, Cambridge, Massachusetts, USA) and Panel 2: cytokeratin (clone AE1/AE3, cat# M351501-2, dilution 1:300, Dako), CD3 (polyclonal, cat#IS503, dilution 1:100, Dako), CD8 (clone C8/144B, cat# MS-457-S, dilution 1:300, Thermo Fisher Scientific), CD45RO (clone UCHL1, cat# PA0146, Cell Signaling Technology), granzyme B (clone 11F1, cat # PA0291, Cell Signaling Technology), and FOXP3 (clone D2W8E, cat# 98377S, Cell Signaling Technology). All the markers were stained in sequence using their respective fluorophore contained in the Opal 7 kit (catalog #NEL797001KT; Akoya Biosciences, Waltham, Massachusetts, USA). Antibody clones and dilutions are the same as were used recently and described.<sup>22</sup> All markers were sequentially applied and stained using their respective fluorophores in the Opal 7 kit (catalog #NEL797001KT; Akoya Biosciences, Waltham, Massachusetts, USA). The slides were scanned using the Vectra/Polaris V.3.0.3 (Akoya Biosciences) at low magnification, 10× (1.0 μm/pixel) through the full emission spectrum and positive tonsil controls from the run staining to calibrate the spectral image scanner protocol.<sup>23</sup> A pathologist selected representative areas inside the tumor using regions of interest for scanning in high magnification by the Phenochart Software image viewer V.1.0.12 (931×698 μm size at resolution 20×) to capture various elements of tissue heterogeneity. Marker colocalization was employed to identify the following cellular subsets: malignant cells (AE1/AE3+); PD-L1-expressing malignant cells (AE1/AE3+PD-L1+); T cells (CD3+); cytotoxic T cells (CD3+CD8+); antigen-experienced T cells (CD3+PD-1+); antigen-experienced cytotoxic T cells (CD3+CD8+PD-1+); macrophages (CD68+); PD-L1-expressing macrophages (CD68+PD-L1+); cytotoxic activated T cells (CD3+CD8+granzyme B+); effector/memory cytotoxic T cells (CD3+CD8+CD45RO+); and regulatory T cells (CD3+CD8-FOXP3+). Densities of each cell phenotype were quantified as the number of cells/mm<sup>2</sup> in tumor nests and tumor stroma. Malignant cells expressing PD-L1 were also expressed in percentages. Data were consolidated using the RStudio V.3.5.3 (Phenopter V.0.2.2 packet, Akoya Biosciences).

#### CyTOF staining of PBMCs

Cytometry by time-of-flight (CyTOF) is a technology that measures the abundance of metal isotope labels on antibodies and other tags (such as peptide-major histocompatibility complex (MHC) tetramers for labeling specific T cells) on single cells using mass spectroscopy. CyTOF

Intracellular Cytokine Staining (ICS) was performed as previously described by Subrahmanyam and Maecker on samples from 11 patients collected longitudinally.<sup>24</sup> Briefly, frozen PBMCs were thawed and washed two times in complete medium (Roswell Park Memorial Institute RPMI medium supplemented with Pen-Strep and L-glutamine). Cell counts were obtained using a Vi-Cell XR cell viability analyzer (Beckman Coulter, Brea, California, USA). 2×10<sup>6</sup> cells per sample were plated in 96-well U-bottom plates. Veri-Cells tagged with 181Ta were reconstituted according to manufacturer's instructions (BioLegend) and spiked in each sample to a ratio of 1:10. All the samples were rested overnight at 37°C, 5% CO<sub>2</sub>. After resting, secretion inhibitors brefeldin A (5 μg/mL) and monensin (5 μg/mL) (Millipore-Sigma, St. Louis, Missouri, USA) were added along with 10 ng/mL phorbol myristic acetate and 1 μg/mL ionomycin (Millipore-Sigma) and anti-CD107a conjugated with 151Eu. All samples were incubated for 4 hours at 37°C. After washes, cells were stained for dead cell discrimination with Cell-ID 103Rh (Fluidigm, South San Francisco, USA) for 15 min at 37°C. Then, we stained the cells for barcoding with combinations of three anti-CD45 antibodies conjugated to 113In, 115In, 194Pt, 195Pt, 196Pt and 198Pt for 30 min, at room temperature. After washing and pooling the cells, we proceeded to the surface staining for 30 min at room temperature prior to fixation with eBioscience Foxp3/Transcription Factor Fixation concentrate (Thermo Fischer Scientific, Waltham, USA) overnight at 4°C. The next day, cells were permeabilized with eBioscience Perm Buffer and intracellular proteins were stained for 1 hour at room temperature. The complete antibody panel is described in online supplemental table 1; the surface antibody cocktail was prepared in advance and kept lyophilized at -20°C. Finally, cells were stained using Cell-ID Intercalator-Ir (Fluidigm) in 1× phosphate buffered saline (Rockland Immunochemicals, Pottstown, Pennsylvania, USA) + 2% paraformaldehyde (PFA, Alfa-Aesar, Thermo Fischer) and kept at 4°C up to 3 days. Prior to CyTOF acquisition, cells were washed two times with staining buffer, three times with milliQ water and resuspended with 1× EQ Four Element Calibration Beads (Fluidigm). After CyTOF acquisition, the data collected were normalized using the Nolan Lab normalizer (<https://github.com/nolanlab/bead-normalization/releases>), deconvoluted with the Zunder Lab Single Cell Debarcoder (<https://github.com/zunderlab/single-cell-debarcoder>) and then analyzed with Cytobank (<https://cytobank.org/>).

#### Olink soluble analyte assay

We performed circulating plasma analyte measurements using proximity extension assay (Olink) in plasma samples from 11 patients collected longitudinally. A series of 92 proteins, such as cytokines and soluble immune checkpoints included in the “immuno-oncology” panel, were measured as previously described, according to manufacturer's instructions.<sup>25</sup> Protein levels were normalized with the use of internal controls and quantified as log<sub>2</sub> protein

**Table 2** Adverse events at least possibly related to treatment (n=19 patients)

	Any grade	Grade 3–4	Grade 5
Any	17 (89.5%)	9 (47.4%)	0 (0.0%)
Serious	7 (36.8%)	6 (31.6%)	0 (0.0%)
Led to discontinuation	1 (5.3%)	0 (0.0%)	0 (0.0%)
Lead to death	0 (0.0%)		0 (0.0%)
>10% of patients			
Fatigue	9 (47.4%)	0 (0%)	0 (0.0%)
Aspartate aminotransferase increased	6 (31.6%)	1 (5.3%)	0 (0.0%)
Blood bilirubin increased	5 (26.3%)	2 (10.5%)	0 (0.0%)
Diarrhea	5 (26.3%)	2 (10.5%)	0 (0.0%)
Rash maculopapular	5 (26.3%)	0 (0%)	0 (0.0%)
Alanine aminotransferase increased	4 (21.1%)	1 (5.3%)	0 (0.0%)
Pruritus	4 (21.1%)	1 (5.3%)	0 (0.0%)
Nausea	4 (21.1%)	0 (0%)	0 (0.0%)
Alkaline phosphatase increased	3 (15.8%)	1 (5.3%)	0 (0.0%)
Anorexia	3 (15.8%)	1 (5.3%)	0 (0.0%)
Hypothyroidism	3 (15.8%)	1 (5.3%)	0 (0.0%)
Anemia	3 (15.8%)	0 (0%)	0 (0.0%)
Arthralgia	3 (15.8%)	0 (0%)	0 (0.0%)
Lipase increased	2 (10.5%)	2 (10.5%)	0 (0.0%)
Adrenal insufficiency	2 (10.5%)	1 (5.3%)	0 (0.0%)
Hyperglycemia	2 (10.5%)	1 (5.3%)	0 (0.0%)
Hypokalemia	2 (10.5%)	1 (5.3%)	0 (0.0%)
Serum amylase increased	2 (10.5%)	1 (5.3%)	0 (0.0%)
Dry skin	2 (10.5%)	0 (0%)	0 (0.0%)
Headache	2 (10.5%)	0 (0%)	0 (0.0%)
Hypotension	2 (10.5%)	0 (0%)	0 (0.0%)
Pain in extremity	2 (10.5%)	0 (0%)	0 (0.0%)
Vomiting	2 (10.5%)	0 (0%)	0 (0.0%)
Weight loss	2 (10.5%)	0 (0%)	0 (0.0%)
Immune-mediated	14 (73.7%)	7 (36.8%)	0 (0.0%)
Aspartate aminotransferase increased	6 (31.6%)	1 (5.3%)	0 (0.0%)
Blood bilirubin increased	5 (26.3%)	2 (10.5%)	0 (0.0%)
Diarrhea	5 (26.3%)	2 (10.5%)	0 (0.0%)
Rash maculopapular	5 (26.3%)	0 (0%)	0 (0.0%)
Alanine aminotransferase increased	4 (21.1%)	1 (5.3%)	0 (0.0%)
Pruritus	4 (21.1%)	1 (5.3%)	0 (0.0%)
Hypothyroidism	3 (15.8%)	1 (5.3%)	0 (0.0%)
Arthralgia	3 (15.8%)	0 (0%)	0 (0.0%)
Lipase increased	2 (10.5%)	2 (10.5%)	0 (0.0%)
Adrenal insufficiency	2 (10.5%)	1 (5.3%)	0 (0.0%)
Serum amylase increased	2 (10.5%)	1 (5.3%)	0 (0.0%)
Hyperthyroidism	1 (5.3%)	1 (5.3%)	0 (0.0%)
Infusion-related reaction	1 (5.3%)	0 (0%)	0 (0.0%)
Pneumonitis	1 (5.3%)	0 (0%)	0 (0.0%)

**Table 3** Best response summary by RECIST V.1.1 (n=19)

Best RECIST response	Response category, N (%)
Confirmed partial response	2 (11)
Stable disease ≥6 months	3 (16)
Stable disease <6 months	4 (21)
Symptomatic deterioration	1 (5)
Progression	8 (42)
Not assessed	1 (5)

expression (“NPX”), which were then used as input for downstream analysis.

#### Differential expression multivariate analysis

To investigate the longitudinal changes in plasma protein changes associated with treatment, we used the following time points: baseline, C2W9, and progression. To carefully quantify the effect of these variables and additional relevant clinical parameters, we used mixed linear models (R package Dream and mle4<sup>26 27</sup>) to model the variances of each covariate. This approach quantifies the effect of covariates such as phase, time points, or treatment, and allows performing comparisons between multiple categories. Each protein Normalized Protein Expression (NPX) value in the Olink assay is considered as an independent variable while phase, time points and treatments are considered as dependent variables. Additionally, this method enables the estimation of multiple random effects, allows the variance terms to vary across proteins,

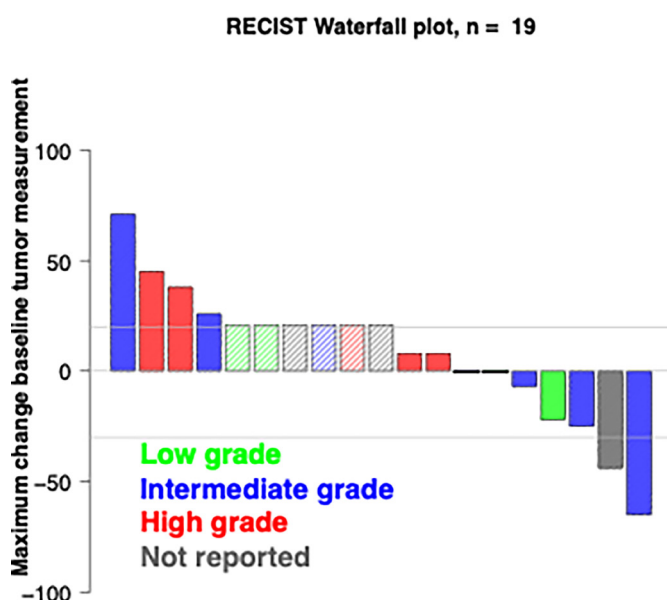


**Figure 1** Waterfall plot of tumor measurements. Gray lines at -30% and 20% indicate lines for partial response and progression per RECIST V.1.1, respectively. Crosshatch-indicated tumor measurements not available due to: progression due to new lesions at first assessment (n=3), death before assessment (n=1), and symptomatic deterioration (n=2).

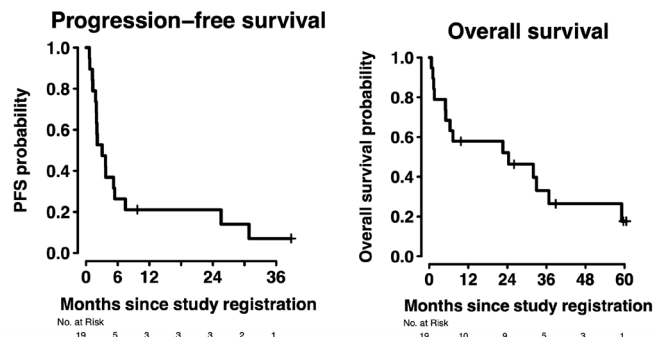


**Figure 2** RECIST V.1.1 progression-free survival and overall survival.

and approximate df of hypothesis test for each protein, thereby minimizing false positive results.

#### Thresholds

To correct for multiple hypothesis testing, we used false discovery rate (FDR) as the preferred method. The thresholds for significance in the mixed linear models for differential expression tests were a log<sub>2</sub> fold change of at least 0.5 and an FDR<0.05. The joint model’s threshold for significance was at least one unit increase in log<sub>2</sub> NPX expression and FDR<0.05.

#### Statistical analysis of translational studies

To evaluate if the baseline biomarkers are prognostically associated with survival, we dichotomized biomarker data by median and performed survival analysis with the log-rank test. To assess if continuous biomarker data are associated with response and other clinical variables, we use non-parametric tests: (1) biomarker versus continuous variable: the Spearman rank correlation; (2) biomarker versus categorical variable with two groups: Mann-Whitney U test; (3) biomarker versus categorical variable with more than two groups: Kruskal-Wallis test. For robust assessment, we also dichotomized biomarker data and used  $\chi^2$  test for response analysis. BH (Benjamini and Hochbert) method was used for multiple-testing adjustment of p values.

## RESULTS

### Patient characteristics

19 patients from 12 National Clinical Trials Network institutions were registered between January 2018 and October 2019 and received protocol therapy, as summarized in table 1. Translational analyses were completed in 2024 and data cut-off as of January 21, 2023. The patients in this cohort are distinct from those in the previously reported cohort.<sup>8 9</sup> The median age was 62 years (range 18–75). Overall, 47% of patients in this cohort were female. Performance status was 0 for 42% of patients, and 58% of patients had an ECOG performance status of 1. The median number of prior lines of therapy was 2. High-grade (grade 3) tumors represented 26% of PNENs in this cohort (N=5 of 19 patients), with 37% being intermediate grade (grade 2), 21% low-grade (grade 1), and with 16%

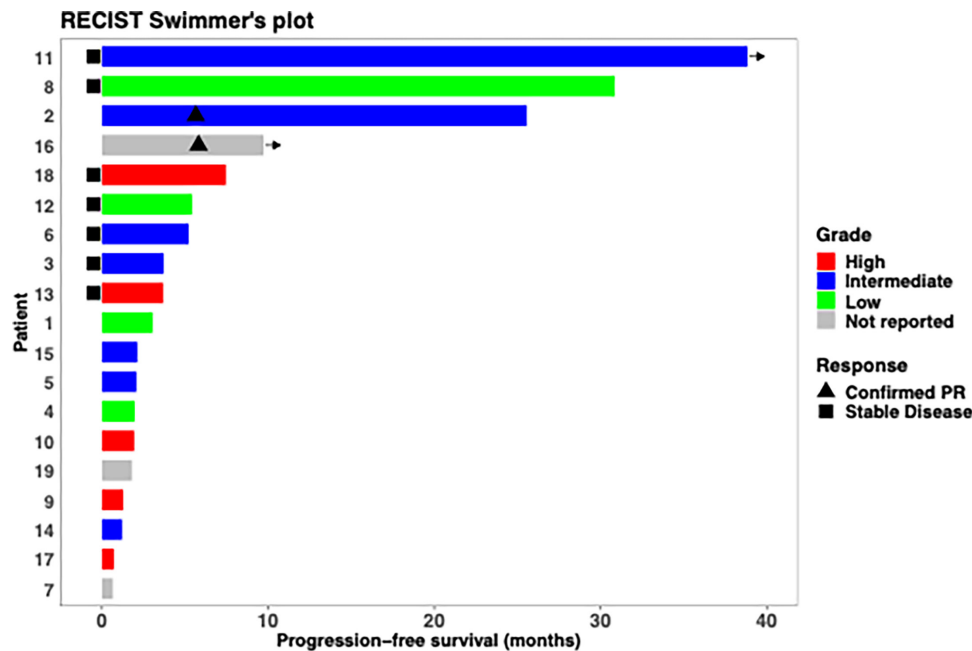


**Figure 3** Swimmer plot (n=19) (see also online supplemental table 2).

of patients with unknown grade. Poorly differentiated tumors represented 10% of patients in this cohort, with 42% well-differentiated and the remainder not reported.

### Toxicities

AEs are summarized in table 2, with 89.5% of patients experiencing an AE on study and ~47% developing a grade 3–4 AE (at least possibly therapy related). There were no grade 5 toxicities reported. The most common toxicities of any grade were fatigue (47%) and AST elevation (32%). The most common immune-mediated toxicity was AST elevation (32%). The most common grade 3/4 AEs were AST elevation, lipase, and total bilirubin elevation (all 11%). The most common immune-related AE was rash (26%), followed by hypothyroidism (16%). No patients discontinued study therapy due to toxicities.

### Clinical outcomes

Among the 19 patients, the ORR was 11% (2 of 19 patients) (95% CI 5% to 40%) and the CBR (SD>6months+PR+CR) was 26% (5 of 19 patients) (95% CI 16% to 62%) (table 3, figure 1). The median PFS was 3 months (95% CI 2 to 26 months) and median overall survival was 24 months (95% CI 6 to  $\infty$  months) (figure 2). Duration of PFS is shown in figure 3, demonstrating durable PFS in some patients with metastatic disease, including in patients with low and intermediate-grade disease; three patients (~16%) have PFS of over 24 months (see also online supplemental table 2). Two patients with a response received treatment for more than 2 years. We also assessed patients with iRECIST, with no reclassification from their RECIST V.1.1 response.

### Analysis of the baseline tumor immune microenvironment

We first investigated the potential relationship between baseline PD-L1 expression, tumor mutation burden and

immune infiltration to determine if there was an association with response or survival. Overall, PD-L1 expression was low with only 1 case out of 12 assessed having appreciable staining above 1% as assessed by a pathologist (figure 4A). The patient with PD-L1 expression had a best response of progressive disease (PD); given the limited number of PD-L1-expressing neoplasms detected in the cohort, the ability to correlate PD-L1 expression with OS or PFS was limited. We further interrogated potential immune infiltration using mIF staining and gene expression profiling. Detection of malignant cells (MC; CK+), as dichotomized by the median counts/mm<sup>2</sup>, was less in patients with clinical benefit (CR+PR+SD>6 months) (online supplemental figure 2A; n=3). Neither the presence of multiple T-cell subsets (CD3+TIL, CD3+CD8+CTLs, CD3+CD8-FoxP3+Tregs), macrophages (CD68+) nor expression of PD-1 or PD-L1 by tumor infiltrating lymphocytes (TILs) or cytotoxic T lymphocytes (CTLs) was associated with response (online supplemental figure 2A). Given the recent findings across multiple tumor types associating B cells with response to immunotherapy approaches, we used gene expression profiling to estimate the frequency of B cells within the tumor immune microenvironment. Stratification of cell scores by median did not show any association with best overall response or clinical benefit (online supplemental figure 2B). Of note, neutrophil cell scores were higher in four out of six patients who did not achieve clinical benefit. However, this analysis is limited as only one patient who achieved clinical benefit was able to be assessed using gene expression profiling. Interestingly, WES showed three out of four cases having a high tumor mutation burden (TMB $\geq$ 10 mutations/mB) and mutations in MHC class II (HLA-DQB1) (figure 4B). High TMB could associate with potential differences in immune infiltration prior



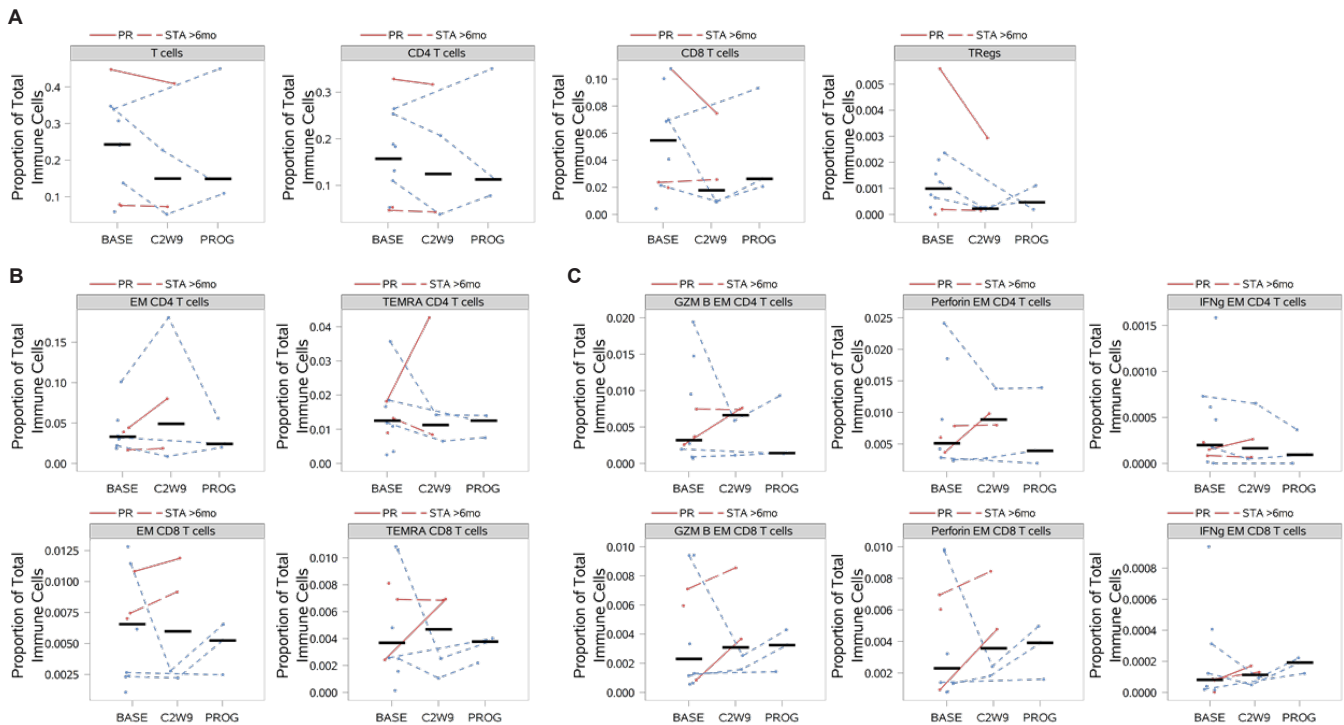


**Figure 5** Increased cytotoxicity profiles in circulation associate with response. Cytometry by time-of-flight profiling of PBMCs after activation with PMA/ionomycin at baseline (base), cycle 2 week 9 (C2W9) and progression (prog) time points. Cell types are graphed as a proportion of total immune cells. Patients with response are shown in red (PR, solid red; SD>6 months, hashed red; n=1 each). Blue dots represent patients with PD or SD<6 months with a hashed line connecting paired longitudinal time points. (A) Changes in frequencies of major T-cell lineages (total T cells, CD4+T cells, CD8+T cells and Tregs) over time are shown with decreases in Tregs observed in PR patient. (B) Memory states in CD4+T cells (top row) and CD8+T cells (bottom row) show expansion of effector memory and TEMRA subsets in PR patient. (C) Cytotoxicity profile as determined by granzyme B (GZMB), perforin and interferon- $\gamma$  production post stimulation within the CD4+effector memory T cells (EM; top row) and CD8+EMT cells (bottom row). Increased expression of granzyme B (GZMB) and perforin is observed in PR patient. C2W9, course 2 week 9; EM, effector memory; PBMC, peripheral blood mononuclear cells; PMA, phorbol myristic acetate; PR, partial response; Prog, progression; SD, stable disease; TEMRA, CD45RA+T cells; Treg, regulatory T cell.

with patient benefit. Analysis of soluble protein changes using Olink was limited to change induced by the combination therapy as all patients except one had a best overall response (BOR) of PD. As expected, soluble PD-1 (PDCD1) increased post-treatment at both C2W9 and progression time points (online supplemental figure 3). The majority of significant protein changes detected were relative to baseline only and levels were maintained between C2W9 and progression, with PDCD1 having the highest induction post-treatment. However, an increase in unique suppressive yet pleiotropic factors such as interleukin-10, carbonic anhydrase IX and heme oxygenase-1 was also observed. These factors have been shown to correlate with disease progression, hypoxia and resistance to immunotherapy-based approaches.<sup>28–32</sup> Circulating cell lineage changes and activation states were assessed using CyTOF at the same time points described above for soluble protein analysis. Statistical changes could not be assessed relative to response as only two patients with samples available for analysis showed benefit to therapy (one PR and one SD>6 months) and the total number of patients was limited. Overall, the frequency of T-cell

subsets (total CD3+, CD4+T cells, CD8+T cells, and Tregs), natural killer cells, B cells, and myeloid cells exhibited patient-specific changes over time, with two out of three PD patients showing a decrease in T-cell subsets including Tregs by C2W9 and the PR patient showing a reduction in CD8+T cells and Tregs by C2W9 (figure 5A and online supplemental figure 4). Increased expression of granzyme B and perforin was observed in a patient with PR. T-cell memory subsets showed stable or reduced frequencies of TEM and TEMRA within the CD4+ and CD8+ T-cell subsets with one PD patient showing expanded memory populations at progression (figure 5B). Interestingly, the patient who achieved a PR showed an increase in T-cell cytotoxic profiles by C2W9 in both CD4+T cell and CD8+T cell subsets, while PD patients showed no change or a reduction in the proportion of circulating immune cells (figure 5C). While anecdotal, this change may highlight an impact of the combination on T-cell activation in PNEN.

## DISCUSSION

PNEN are a histologically heterogeneous group of tumors distinct from pancreatic adenocarcinoma, with

the former arising from endocrine (islet) cells in the pancreas.<sup>33–35</sup> Systemic treatment options for PNENs typically include somatostatin analogs, everolimus, sunitinib, or chemotherapy (temozolomide+capecitabine).<sup>36–39</sup> Historically, the effect of immunotherapy in PNENs is less clear.<sup>40</sup> Prior studies of anti-PD-1 monotherapy have had limited activity in PNENs with ORR~6%.<sup>41–42</sup> The role of anti-CTLA-4 in addition to anti-PD-1 had not previously been rigorously explored in this setting. For S1609 DART, the dose of ipilimumab of 1 mg/kg intravenously every 6 weeks continuous with nivolumab was chosen on balance of toxicity and efficacy, and based on the results of Check-Mate 227.<sup>43</sup> This dosing combination of ipilimumab and nivolumab has also become one of the frontline standards of care for metastatic non-small cell lung cancer.<sup>44</sup>

Another recently published immunotherapy basket study, CA209-538, included ipilimumab with a different dosing schema (1 mg/kg every 3 weeks for four doses) in combination with nivolumab every 2 weeks.<sup>45</sup> In this study, PNEN had an ORR of 43% (3/7), though these were all with high-grade neoplasms (differentiation status unclear), including a patient who had disease progression on prior anti-PD-1. There were two patients with poorly differentiated pancreatic neuroendocrine carcinomas (NEC) and five with well-differentiated pancreatic neuroendocrine tumors (NET). Of these, one pancreatic NEC and two grade 3 pancreatic NET had a PR. The KEYNOTE-028 study included patients with well-differentiated PNENs with PD-L1>1% expression by 22C3 and 16 patients were ultimately treated with pembrolizumab for an ORR of 6.3%.<sup>41</sup> In our current study, the ORR was 11% (2/19 patients); the CBR (SD>6months+PR+CR), 26% (5/19); only five patients had high-grade disease and only two patients had poorly differentiated disease (table 1).

Biomarker analyses showed that most patients did not express high levels of PD-L1; indeed, only 1 case out of 12 assessed had appreciable staining above 1% (and that patient had a best response of PD). One of three patients with a high TMB achieved an objective response and this patient had a very high TMB of~150 mutations/mB (PFS was 26 months). Peripheral immune analyses suggested that activated effector and helper T cells and reduced Treg and myeloid cells may be associated with therapeutic response, but numbers were limited in our analysis; these parameters merit further prospective investigation.

Limitations of this study include its lack of central pathology or radiology review, no randomized comparator, and small sample size. Tumor grading and histologic assessment were performed locally where the rarity of the tumor and pathologic heterogeneity may be more variable. Additionally, there was no central radiology review of CTs, and local imaging response assessments were used for the primary endpoint of ORR with RECIST V.1.1. Finally, the number of patients available for biomarker analyses was limited. Specifically, there are only a small number of patients with high

TMB or intermediate-grade tumors—additional studies are warranted before definitive conclusions can be made regarding the role of these factors in predicting response to dual immunotherapy.

In summary, herein we describe a dedicated PNEN cohort of SWOG 1609 assessing low-dose ipilimumab plus nivolumab. We demonstrate modest activity in a subset of patients with PNEN. Toxicities on this study were manageable with no grade 5 events. An 11% PR rate and an overall 26% CBR (includes ORR and SD>6 months) indicate that a subset of patients received the majority of benefit in this study, with 3/19 patients remaining progression-free for over 2 years in this refractory setting. Interestingly, while the majority of the benefit was in high-grade PNETs, a subset of responding patients harbored intermediate or low-grade tumors, which generally did not show benefit in our other cohorts of neuroendocrine tumors treated with nivolumab and ipilimumab. This recapitulates our experience in non-pancreatic neuroendocrine cohorts, where almost all benefit was in high-grade cancers.<sup>8–9</sup> Future studies identifying the relevant immunobiologic characteristics that are associated with tumor grade and immunotherapeutic response across neuroendocrine subtypes are warranted, and combinatorial strategies are a potential opportunity for patients with this rare tumor type.

#### Author affiliations

<sup>1</sup>UC San Diego Health Moores Cancer Center, La Jolla, California, USA

<sup>2</sup>University of Washington, Seattle, Washington, USA

<sup>3</sup>Hematology and Oncology, Northwestern University Feinberg School of Medicine, Chicago, Illinois, USA

<sup>4</sup>Translational Molecular Pathology, University of Texas MD Anderson Cancer Center, Houston, Texas, USA

<sup>5</sup>KUMC, Kansas City, Kansas, USA

<sup>6</sup>Internal Medicine, Division Of Medical Oncology, The Ohio State University, Columbus, Ohio, USA

<sup>7</sup>Cancer Care Center of O'Fallon, O'Fallon, Illinois, USA

<sup>8</sup>Department of Bioinformatics and Computational Biology, University of Texas MD Anderson Cancer Center, Houston, Texas, USA

<sup>9</sup>Institute for Immunity, Transplantation, Infections, Stanford University School of Medicine, Stanford, California, USA

<sup>10</sup>Precision Immunology Institute and Tisch Cancer Institute, Department of Immunology, Icahn School of Medicine at Mount Sinai, New York, New York, USA

<sup>11</sup>University of Texas MD Anderson Cancer Center, Houston, Texas, USA

<sup>12</sup>Department of Genomic Medicine, The University of Texas MD Anderson Cancer Center, Houston, Texas, USA

<sup>13</sup>Icahn School of Medicine at Mount Sinai, New York, New York, USA

<sup>14</sup>Stanford University School of Medicine, Stanford, California, USA

<sup>15</sup>Medicine - Hem/Onc, Icahn School of Medicine at Mount Sinai, New York, New York, USA

<sup>16</sup>Thoracic Medical Oncology, University of Texas MD Anderson Cancer Center, Houston, Texas, USA

<sup>17</sup>SWOG, San Antonio, Texas, USA

<sup>18</sup>CTEP, National Cancer Institute, Bethesda, Maryland, USA

<sup>19</sup>National Cancer Institute, Bethesda, Maryland, USA

<sup>20</sup>Fred Hutchinson Cancer Research Center, Seattle, Washington, USA

<sup>21</sup>OHSU, Portland, Oregon, USA

<sup>22</sup>Medical College of Wisconsin, Milwaukee, Wisconsin, USA

X Sandip Pravin Patel @PatelOncology, Edgar Gonzalez-Kozlova @EdgarEGK, Helen X Chen @Helen Chen and Cara L Haymaker @cara\_haymaker

**Acknowledgements** The authors wish to thank Ms Marcia Horn, JD, SWOG Patient Advocate and President/CEO, ICAN-International Cancer Advocacy Network; Ms Christy Klepetko, Protocol Coordinator, SWOG Operations Office; Dr Howard Streicher, MD, National Cancer Institute, Investigational Drug Branch, Cancer Therapy Evaluation Program. We thank all the members of the CIMAC sites for their contribution to the sample and assay logistics and support; specifically, Julia Mendoza Perez, Dawen Sui, Diane Del Valle, Kai Nie, Jingjing Qi and Mina Pichavang. We also thank the CIDC members Len Taing and Jacob Geisberg for their work on WES and genomics, and Kristen Anton, Stephen Van Nostrand, James Provencher, Jennifer Altreuter, Joyce Yu, Ethan Cerami, and Franziska Michor for data curation and leadership. The authors would also like to thank the National Cancer Institute Project Managers for their work supporting the CIMAC-CIDC correlative study.

**Contributors** SP is guarantor. SP, YKC, and RK co-equal corresponding authors.

**Funding** RK is funded in part by 5U01CA180888-08 and 5UG1CA233198-05. SG is partially supported by NIH grants U01DK124165, R33CA263705, and P30CA196521. This work was supported by the National Institutes of Health, National Cancer Institute grant awards CA180888, CA180819, CA180821, CA233331, CA233320, CA180828; and in part by Bristol-Myers Squibb Company. The content is solely the responsibility of the authors and does not necessarily represent the official views of the National Institutes of Health. Scientific and financial support for the Cancer Immune Monitoring and Analysis Centers-Cancer Immunologic Data Center (CIMAC-CIDC) Network are provided through the National Cancer Institute (NCI) Cooperative Agreements, U24CA224319 (to the Icahn School of Medicine at Mount Sinai CIMAC), U24CA224285 (to the MD Anderson Cancer Center CIMAC), U24CA224309 (to the Stanford University CIMAC), and U24CA224316 (to the CIDC at Dana-Farber Cancer Institute), and through NCI contract 140D0421D0007 to the CIDC operated by NCI.

**Competing interests** RK has received research funding from Boehringer Ingelheim, Debiopharm, Foundation Medicine, Genentech, Grifols, Guardant, Incyte, Konica Minolta, Medimmune, Merck Serono, Omiseq, Pfizer, Sequenom, Takeda, and TopAlliance and from the NCI; as well as consultant and/or speaker fees and/or advisory board/consultant for Actuate Therapeutics, AstraZeneca, Bicara Therapeutics, Inc., Biological Dynamics, Caris, Datar Cancer Genetics, Daiichi, Eisai, EOM Pharmaceuticals, Iylon, LabCorp, Merck, NeoGenomics, Neomed, Pfizer, Precirix, Prosperdx, Regeneron, Roche, TD2/Volastra, Turning Point Therapeutics, X-Biotech; has an equity interest in CureMatch Inc.; serves on the Board of CureMatch and CureMetrix, and is a co-founder of CureMatch. CWR received grants through his institution from Ayala, Bristol-Meyer Squibb, Daiichi-Sankyo, Deciphera, Exelixis, Genentech, Novartis, Karyopharm Therapeutics, Merck, Nektar, Pfizer, Xynomic, PF Argentum IP Holdings LLC, Rain Therapeutics, Shasqi, PTC Therapeutics, NiKang Therapeutics; consulting fees from Synox, Daiichi Sankyo, AVEO, Exelixis, Astra Zeneca, Bristol-Meyer Squibb; payment for expert testimony from Pfizer, GSK, Boehringer Ingelheim. JLL received partial funding from CA016672 from National Cancer Institute. IIW received consulting fees from Caris Life Sciences - Virtual molecular tumor board; payments from Advisory boards for AstraZeneca, Daiichi Sankyo, Takeda, Novartis, EMD Serono, Janssen, Pfizer, Eli Lilly and Company, Bayer, Regeneron, BMS and Genentech. Payment as Speaker from Blueprint Medicines, Janssen, Mirati and Takeda; support for attending meetings/travel from AnHeart Therapeutics; stock or stock options from MBrace Therapeutics. SP received grants or contracts from Amgen, AstraZeneca, A2bio, Bristol-Myers Squibb, Eli Lilly, Fate Therapeutics, Gilead, Iovance, Merck, Pfizer, Roche/Genentech; consulting fees from Amgen, AstraZeneca, BeiGene, Bristol-Myers Squibb, Eli Lilly, Genentech, Merck, Pfizer, Zai Labs. ES received consulting fees from D.E. Shaw Research; participated on a Data Safety Monitoring Board or Advisory Board for Mallinckrodt Pharmaceuticals. AK received grants or contracts through institution from TESARO, Astellas Pharma, Rafael Pharmaceuticals, Geistlich Pharma, Cardiff Oncology, FibroGen, Bavarian Nordic, Novocure, Cend Therapeutics, Ability Pharma, Novita, Boundless Bio; consulting fees from Ipsen; Payment or honoraria for lectures, presentations, speakers bureaus, manuscript writing or educational events from Cardinal Health; Participation on a Data Safety Monitoring Board or Advisory Board for Ipsen. CLH received grants or contracts through institution from Sanofi, Avenge, Iovance, KSQ, Dragonfly, BTG, Novartis, 280Bio/Yingli, 4D Pharma, Medimmune/AZ, EMD Serono/Merck, Takeda, Obsidian, Genentech, BMS, Summit Therapeutics, Artidis, Immunogenesis; consulting fees from Regeneron; support for travel from Society for Immunotherapy of Cancer; Patents planned, issued or pending 62/977, 672 Managed by institution; stock or stock options from Briacell. DYD reports support from NIH CIMAC grant through institution; speaker honorarium from One Lambda. BK reported grant or contract through institution from Merck, Eisai, Xencor (ended in 8/2022). SG reports grant or contract from Boehringer Ingelheim, Bristol-Myers Squibb, Celgene, Genentech,

Regeneron, and Takeda (Not as PI, payment to Institution, unrelated); consulting fee from Taiho Pharmaceuticals. MO reports support from NIH/NCI grant U10CA180819. HTM reports support from NIAID through institution and from Bill & Melinda Gates Foundation through institution; royalties or licenses from Standard BioTools; support for attending meetings/travel from Alamar Biosciences, Curiox Biosciences; Profiling and Treatment of MYC-Associated Cancers; Patents planned, issued or pending: U.S. Patent 11,648,275; SITC Biomarkers Committee - Leadership or fiduciary role in other board, society, committee or advocacy group, paid or unpaid; stock or stock options from BD Biosciences Cytek, Inc. JZ reports support from National Cancer Institute of the National Institute of Health Research Project Grant (R01CA234629), the AACR-Johnson & Johnson Lung Cancer Innovation Science Grant (18-90-52-ZHAN), the MD Anderson Physician Scientist Program, MD Anderson Lung Cancer Moon Shot Program; consulting fees from Johnson and Johnson, AstraZeneca, Novartis; Payment or honoraria for lectures, presentations, speakers bureaus, manuscript writing or educational events from Novartis, Bristol Myers Squibb, AstraZeneca, GenePlus, Innovent and Hengrui, St. Lucia, BeiGene; Participation on a Data Safety Monitoring Board or Advisory Board for Novartis, AstraZeneca, GenePlus, Catalyst, Heliuss, Oncohost, St Lucia; Receipt of equipment, materials, drugs, medical writing, gifts or other services from Novartis, Johnson and Johnson, Merck, Summit, Heliuss.

**Patient consent for publication** Not applicable.

**Ethics approval** This study involves human participants and was approved by The NCI Central Institutional Review Board (CIRB). The NCI Central Institutional Review Board (CIRB) does not use study number and is identified as S1609 by CIRB. Participants gave informed consent to participate in the study before taking part.

**Provenance and peer review** Not commissioned; externally peer reviewed.

**Data availability statement** All data relevant to the study are included in the article or uploaded as supplementary information.

**Supplemental material** This content has been supplied by the author(s). It has not been vetted by BMJ Publishing Group Limited (BMJ) and may not have been peer-reviewed. Any opinions or recommendations discussed are solely those of the author(s) and are not endorsed by BMJ. BMJ disclaims all liability and responsibility arising from any reliance placed on the content. Where the content includes any translated material, BMJ does not warrant the accuracy and reliability of the translations (including but not limited to local regulations, clinical guidelines, terminology, drug names and drug dosages), and is not responsible for any error and/or omissions arising from translation and adaptation or otherwise.

**Open access** This is an open access article distributed in accordance with the Creative Commons Attribution Non Commercial (CC BY-NC 4.0) license, which permits others to distribute, remix, adapt, build upon this work non-commercially, and license their derivative works on different terms, provided the original work is properly cited, appropriate credit is given, any changes made indicated, and the use is non-commercial. See <http://creativecommons.org/licenses/by-nc/4.0/>.

#### ORCID iDs

Sandip Pravin Patel <http://orcid.org/0000-0002-8387-4840>  
 Young Kwang Chae <http://orcid.org/0000-0003-1557-7235>  
 Caroline Duault <http://orcid.org/0000-0003-2742-1668>  
 J Jack Lee <http://orcid.org/0000-0001-5469-9214>  
 Jianjun Zhang <http://orcid.org/0000-0001-7872-3477>  
 Megan Othus <http://orcid.org/0000-0001-8176-6371>  
 Cara L Haymaker <http://orcid.org/0000-0002-1317-9287>

#### REFERENCES

- Morris VK, Salem ME, Nimeiri H, *et al*. Nivolumab for previously treated unresectable metastatic anal cancer (NCI9673): a multicentre, single-arm, phase 2 study. *Lancet Oncol* 2017;18:446–53.
- Nghiem PT, Bhatia S, Lipson EJ, *et al*. PD-1 Blockade with Pembrolizumab in Advanced Merkel-Cell Carcinoma. *N Engl J Med* 2016;374:2542–52.
- Wagner MJ, Othus M, Patel SP, *et al*. Multicenter phase II trial (SWOG S1609, cohort 51) of ipilimumab and nivolumab in metastatic or unresectable angiosarcoma: a substudy of dual anti-CTLA-4 and anti-PD-1 blockade in rare tumors (DART). *J Immunother Cancer* 2021;9:e002990.
- Adams S, Othus M, Patel SP, *et al*. A Multicenter Phase II Trial of Ipilimumab and Nivolumab in Unresectable or Metastatic Metaplastic Breast Cancer: Cohort 36 of Dual Anti-CTLA-4 and Anti-PD-1

- Blockade in Rare Tumors (DART, SWOG S1609). *Clin Cancer Res* 2022;28:271–8.
- 5 Chae YK, Othus M, Patel S, *et al.* A phase II basket trial of dual anti-CTLA-4 and anti-PD-1 blockade in rare tumors (DART) SWOG S1609: the thyroid tumor cohort. *J Immunother Cancer* 2020;8:A161–A61.
  - 6 Chae YK, Othus M, Patel SP, *et al.* Abstract 3417: A phase II basket trial of dual anti-CTLA-4 and anti-PD-1 blockade in rare tumors (DART) SWOG S1609: The small bowel tumor cohort. *Cancer Res* 2020;80:3417.
  - 7 Chae YK, Othus M, Patel SP, *et al.* Abstract 3418: A phase II basket trial of dual anti-CTLA-4 and anti-PD-1 blockade in rare tumors (DART) SWOG S1609: The salivary gland tumor cohort. *Cancer Res* 2020;80:3418.
  - 8 Patel SP, Othus M, Chae YK, *et al.* A Phase II Basket Trial of Dual Anti-CTLA-4 and Anti-PD-1 Blockade in Rare Tumors (DART SWOG 1609) in Patients with Nonpancreatic Neuroendocrine Tumors. *Clin Cancer Res* 2020;26:2290–6.
  - 9 Patel SP, Mayerson E, Chae YK, *et al.* A phase II basket trial of Dual Anti-CTLA-4 and Anti-PD-1 Blockade in Rare Tumors (DART) SWOG S1609: High-grade neuroendocrine neoplasm cohort. *Cancer* 2021;127:3194–201.
  - 10 DeSantis CE, Kramer JL, Jemal A. The burden of rare cancers in the United States. *CA Cancer J Clin* 2017;67:261–72.
  - 11 Brookmeyer R, Crowley J. A k-Sample Median Test for Censored Data. *J Am Stat Assoc* 1982;77:433.
  - 12 Koyama T, Chen H. Proper inference from Simon's two-stage designs. *Stat Med* 2008;27:3145–54.
  - 13 McKenna A, Hanna M, Banks E, *et al.* The Genome Analysis Toolkit: a MapReduce framework for analyzing next-generation DNA sequencing data. *Genome Res* 2010;20:1297–303.
  - 14 Kendig KI, Baheti S, Bockol MA, *et al.* Sentieon DNaseq Variant Calling Workflow Demonstrates Strong Computational Performance and Accuracy. *Front Genet* 2019;10:736.
  - 15 McLaren W, Gil L, Hunt SE, *et al.* The Ensembl Variant Effect Predictor. *Genome Biol* 2016;17:122.
  - 16 Talevich E, Shain AH, Botton T, *et al.* CNVkit: Genome-Wide Copy Number Detection and Visualization from Targeted DNA Sequencing. *PLoS Comput Biol* 2016;12:e1004873.
  - 17 Favero F, Joshi T, Marquard AM, *et al.* Sequenza: allele-specific copy number and mutation profiles from tumor sequencing data. *Ann Oncol* 2015;26:64–70.
  - 18 Shen R, Seshan VE. FACETS: allele-specific copy number and clonal heterogeneity analysis tool for high-throughput DNA sequencing. *Nucleic Acids Res* 2016;44:e131.
  - 19 Gillis S, Roth A. PyClone-VI: scalable inference of clonal population structures using whole genome data. *BMC Bioinformatics* 2020;21:571.
  - 20 Roth A, Khattra J, Yap D, *et al.* PyClone: statistical inference of clonal population structure in cancer. *Nat Methods* 2014;11:396–8.
  - 21 Parra ER, Villalobos P, Mino B, *et al.* Comparison of Different Antibody Clones for Immunohistochemistry Detection of Programmed Cell Death Ligand 1 (PD-L1) on Non-Small Cell Lung Carcinoma. *Appl Immunohistochem Mol Morphol* 2018;26:83–93.
  - 22 Parra ER, Ferrufino-Schmidt MC, Tamegnon A, *et al.* Immunoprofiling and cellular spatial analysis using five immune oncology multiplex immunofluorescence panels for paraffin tumor tissue. *Sci Rep* 2021;11:8511.
  - 23 Parra ER, Jiang M, Solis L, *et al.* Procedural Requirements and Recommendations for Multiplex Immunofluorescence Tyramide Signal Amplification Assays to Support Translational Oncology Studies. *Cancers (Basel)* 2020;12:255.
  - 24 Subrahmanyam PB, Maecker HT. CyTOF Measurement of Immunocompetence Across Major Immune Cell Types. *Curr Protoc Cytom* 2017;82:9.
  - 25 Monjazeb AM, Giobbie-Hurder A, Lako A, *et al.* A Randomized Trial of Combined PD-L1 and CTLA-4 Inhibition with Targeted Low-Dose or Hypofractionated Radiation for Patients with Metastatic Colorectal Cancer. *Clin Cancer Res* 2021;27:2470–80.
  - 26 Hoffman GE, Schadt EE. variancePartition: interpreting drivers of variation in complex gene expression studies. *BMC Bioinformatics* 2016;17:483.
  - 27 Bolker B, Walker S. Fitting linear mixed-effects models using lme4. *J Stat Softw* 2015;67:1–48.
  - 28 Chiang SK, Chen SE, Chang LC. The Role of HO-1 and Its Crosstalk with Oxidative Stress in Cancer Cell Survival. *Cells* 2021;10:2401.
  - 29 Alaluf E, Vokaer B, Detavernier A, *et al.* Heme oxygenase-1 orchestrates the immunosuppressive program of tumor-associated macrophages. *JCI Insight* 2020;5:e133929.
  - 30 Sun Z, Fourcade J, Pagliano O, *et al.* IL10 and PD-1 Cooperate to Limit the Activity of Tumor-Specific CD8+ T Cells. *Cancer Res* 2015;75:1635–44.
  - 31 Gautam SK, Batra SK, Jain M. Molecular and metabolic regulation of immunosuppression in metastatic pancreatic ductal adenocarcinoma. *Mol Cancer* 2023;22:118.
  - 32 Ward C, Meehan J, Gray M, *et al.* Carbonic Anhydrase IX (CAIX), Cancer, and Radiation Responsiveness. *Metabolites* 2018;8:13.
  - 33 Burns WR, Edil BH. Neuroendocrine pancreatic tumors: guidelines for management and update. *Curr Treat Options Oncol* 2012;13:24–34.
  - 34 Maharjan CK, Ear PH, Tran CG, *et al.* Pancreatic Neuroendocrine Tumors: Molecular Mechanisms and Therapeutic Targets. *Cancers (Basel)* 2021;13:5117.
  - 35 Yang KC, Kalloger SE, Aird JJ, *et al.* Proteotranscriptomic classification and characterization of pancreatic neuroendocrine neoplasms. *Cell Rep* 2021;37:109817.
  - 36 Stueven AK, Kayser A, Wetz C, *et al.* Somatostatin Analogues in the Treatment of Neuroendocrine Tumors: Past, Present and Future. *Int J Mol Sci* 2019;20:3049.
  - 37 Yao JC, Shah MH, Ito T, *et al.* Everolimus for advanced pancreatic neuroendocrine tumors. *N Engl J Med* 2011;364:514–23.
  - 38 Raymond E, Dahan L, Raoul J-L, *et al.* Sunitinib malate for the treatment of pancreatic neuroendocrine tumors. *N Engl J Med* 2011;364:501–13.
  - 39 Vaghaiwalla T, Memeh K, Liao C-Y, *et al.* Metastatic well-differentiated pancreatic neuroendocrine tumors to the liver: a narrative review of systemic and surgical management. *J Pancreatol* 2021;4:82–9.
  - 40 Yao JC, Strosberg J, Fazio N, *et al.* 1308OActivity & safety of spartalizumab (PDR001) in patients (pts) with advanced neuroendocrine tumors (NET) of pancreatic (Pan), gastrointestinal (GI), or thoracic (T) origin, & gastroenteropancreatic neuroendocrine carcinoma (GEP NEC) who have progressed on prior treatment (Tx). *Ann Oncol* 2018;29.
  - 41 Mehnert JM, Bergsland E, O'Neil BH, *et al.* Pembrolizumab for the treatment of programmed death-ligand 1-positive advanced carcinoid or pancreatic neuroendocrine tumors: Results from the KEYNOTE-028 study. *Cancer* 2020;126:3021–30.
  - 42 Strosberg J, Mizuno N, Doi T, *et al.* Efficacy and Safety of Pembrolizumab in Previously Treated Advanced Neuroendocrine Tumors: Results From the Phase II KEYNOTE-158 Study. *Clin Cancer Res* 2020;26:2124–30.
  - 43 Hellmann MD, Ciuleanu T-E, Pluzanski A, *et al.* Nivolumab plus ipilimumab in Lung Cancer with a High Tumor Mutational Burden. *N Engl J Med* 2018;378:2093–104.
  - 44 Paz-Ares L, Ciuleanu T-E, Cobo M, *et al.* First-line nivolumab plus ipilimumab combined with two cycles of chemotherapy in patients with non-small-cell lung cancer (CheckMate 9LA): an international, randomised, open-label, phase 3 trial. *Lancet Oncol* 2021;22:198–211.
  - 45 Klein O, Kee D, Markman B, *et al.* Immunotherapy of Ipilimumab and Nivolumab in Patients with Advanced Neuroendocrine Tumors: A Subgroup Analysis of the CA209-538 Clinical Trial for Rare Cancers. *Clin Cancer Res* 2020;26:4454–9.